Journal of Macromolecular Science, Part A
Publication details, including instructions for authors and subscription information:
http://www.informaworld.com/smpp/title~content=t713597274

Fluorescence Studies on Thiol-Functional Polystyrene-CdS Nanocomposites

Yanmao Dong[a]; Jianmei Lu[a]; Qingfeng Xu[a]
[a] School of Chemistry and Chemical Engineering, Soochow University, Suzhou, China

To cite this Article Dong, Yanmao , Lu, Jianmei and Xu, Qingfeng(2008) 'Fluorescence Studies on Thiol-Functional Polystyrene-CdS Nanocomposites', Journal of Macromolecular Science, Part A, 45: 1, 37 — 43
To link to this Article: DOI: 10.1080/10601320701681920
URL: http://dx.doi.org/10.1080/10601320701681920

Journal of Macromolecular Science®, Part A: Pure and Applied Chemistry (2008) **45**, 37–43

ISSN: 1060-1325 print/1520-5738 online
DOI: 10.1080/10601320701681920

Fluorescence Studies on Thiol-Functional Polystyrene-CdS Nanocomposites

YANMAO DONG, JIANMEI LU, and QINGFENG XU

School of Chemistry and Chemical Engineering, Soochow University, Suzhou, China

Received May, 2007, Accepted June, 2007

Thiol-functional polystyrene-CdS nanocomposites have been prepared via an *in-situ* method. The products were characterized in detail. The photoluminescence properties of products were also studied. The thiol fraction in thiol-functional polystyrene can be controlled by the copolymerization of styrene and 4-chloromethylstyrene. So, the CdS content in polymer and the photoluminescence properties of nanocomposites can be tuned up quantificationally. Results show that the fluorescence of nanocomposites depends on the CdS content. The charge-transfer mechanism of nanocomposites accords with ligand-to-metal charge-transfer (LMET) model. These nanocomposites can be used as potential optical materials.

Keywords: thiol; polystyrene; CdS; nanocomposites; fluorescence

1 Introduction

Monodispersed nano CdS can be prepared by covering the surface with polymer (1–3). CdS nanocrystals embedded in polymers have been widely studied (4–13). The fluorescent performance of nano CdS can also be drastically improved. As stabilizing agents and capping ligands, the presence of different thiols (thioethanol, thioglycerol, thioglycolic acid, dithioglycerol, mercaptoethylamine, L-cysteine, etc.) allows control over the nano-particle size. Takayuki Hirai et al. (14) reported the introduction of a poly-(ethylene glycol) (PEG) chain between the thiol group and the polystyrene can enhance the percentage immobilization of CdS. The wavelength region of photoabsorption was controlled easily and precisely. In other literature (15), the PL spectra of thiol-functional poly(caprolactone)/CdS (PCL-SH/CdS) showed red-shift with a increasing particle size. Control of CdS content is one of the key factors to tune up the optical property of the nanocomposites. The charge-transfer mechanism between the polymer and nano CdS also should be studied further.

In the present work, we address the synthesis of thiol-functional polystyrene (TPS)-CdS nanocomposites (TPSC) by an *in-situ* method. The nanocomposites have been characterized and the fluorescent properties have been studied in detail. The polymer and nanocomposites were affirmed by FT-IR, FT-Raman, NMR, XRD, XPS, DSC, ICP, SEM and TEM. The CdS content has been controlled by the thiol-to-$CdCl_2$ ratio. The effects of CdS content and excited wavelength on photoluminescence (PL) performance of TPSC have been discussed. The charge-transfer model of TPSC also was delivered.

Address correspondence to: Jianmei Lu, School of Chemistry and Chemical Engineering, Soochow University, Suzhou 215123, China. Fax: + 8651265882875; E-mail: lujm@suda.edu.cn

2 Experimental

2.1 Materials

All the reactants and solvents used in this study were analytical grade. Styrene and 4-chloromethylstyrene (Aldrich) was vacuum distilled from CaH immediately prior to polymerization. All others reagents and solvents were used as received.

2.2 Preparation of TPS

Polystyrene-*co*-polychloromethylstyrene were prepared as follows: An DMF solution (100 mL) containing of 2.15 g (14.1 mmol) 4-chloromethylstyrene, and 142 mg (0.86 mmol) of 2,2-azobis(isobutyronitrile) (AIBN) was stirred gently at 343 K and under N_2 over a period of 24 h. The polymer obtained were washed with methanol and dried *in vacuo* overnight. TPS with a different amount of thiol was prepared according to the procedure reported by Garamszegi et al. (16).

2.3 In-situ Synthesis of TPSC

5 mmol $CdCl_2 \cdot 2.5H_2O$ was added to a 20 mL N,N′-dimethylformamide DMF solution containing TPS (thiol fraction was 5 mmol) and the mixture stirred by magnetic stirrer at 298 K in a glass vessel for 24 h. The TPS-Cd^{2+} obtained was washed with methanol and extracted by an Soxhlet extractor (methanol:water = 1:1,v:v) for 48 h. The purified products were dried *in vacuo* overnight.

0.2 g TPS-Cd^{2+} containing 5 mmol Cd^{2+} reacted with 5.5 mmol $Na_2S \cdot 9H_2O$ in 20 mL DMF solution at 298 K for 1 h. The nano-CdS was observed during stirring and ultrasound dispersion. The resulting TPSC obtained was washed with methanol and distilled water, and dried at room temperature. Other TPSC with different a TPS-to-Cd^{2+}ratio has been prepared using the same process.

2.4 Characterization

Fourier transform infrared spectroscopy (FT-IR) was measured to characterize the composition of the copolymer and the copolymer-CdS composite using a Nicolet MagNa-IR550 FTIR spectrophotometer. All samples were recorded in KBr discs.

The FT-Raman spectra were excited by 1064 nm line of an Nd:YVO_2 laser. We used a Nicolet FT-Raman 960 monochromator with a conventional photocounting system.

^{1}H-NMR spectra were recorded in DMSO on a Inova-400 instrument using tetra-order methylsilane as a reference.

The associated elemental composition was determined by using a Hitachi S-570 Scanning Electron Microscope (SEM) equipped with Energy Dispersive Analysis by an X-rays (EDAX) facility.

The size and shape of the nanoparticles were determined by a Hitachi H-600-II transmission electron microscope (TEM).

The Z-average size and the polydispersity index (PDI) of the nanocomposites were measured by a Malvern HPP 5001 high performance particle sizer (HPPS) at 20°C.

The CdS content in these composites were investigated by means of Inductively Coupled Plasma (ICP) (PLA-SPECI, Leeman Company). Samples for ICP were prepared by dispersing the product in 98% HNO_3 and then boiling it for 30 min. The solution containing Cd was diluted with distilled water.

The X-ray diffraction (XRD) patterns were recorded on a Rigaku D/MAX-IIIC X-ray diffractometer using Cu Ka radiation ($\lambda = 0.1542$ nm) operated at 50 kV and 100 mA. The experiments were performed in the range of the diffraction angle $2\theta = 5-70^\circ$.

The X-ray photoelectron spectroscopy (XPS) data were accumulated on an VG ESCA LAB MK-electron spectrometer system with a monochromatized Al(Kα) (h = 1486.6 eV, 10.0 kV) standard X-ray source. The binding energies were calibrated by referencing the C(1s) to 285.0 eV.

The stability of these complexes were investigated by means of differential scanning calorimetry (DSC) using a TA DSC 2010. The samples were examined at a scanning rate of 10 K min^{-1} by applying two heating and one cooling cycle.

Ultraviolet-Visible (UV-Vis) absorption spectroscopy of the samples were recorded on a Shimadzu UV-Vis spectrophotometer (UV-2401PC), by scanning the composite-containing solution in a 1-cm quartz cell. The scanning range was from 190 to 700 nm. Absorption from the solvent was subtracted from each spectrum.

The fluorescence spectra of products were obtained on an Shimadzu Edinburgh-920 spectrophotometer equipped with a 450-W Xe arc lamp and a PMT detector at room temperature.

3 Results and Discussion

3.1 Preparation of TPSC

Figure 1 shows the synthesis of the TPS and *in-situ* preparation of TPSC nanocomposites.

3.2 FT-IR Spectra

The copolymerization of St and chloromethylstyrene can be confirmed from the FT-IR spectra. Figure 2 shows the spectra of the polystyrene-*co*-polychloromethylstyrene, TPS and TPSC. The FT-IR spectrum of polystyrene-*co*-polychloromethylstyrene shows a strong characteristic C-Cl stretching band at 740 cm^{-1} in Fig. 2(a). The spectrum of the TPS sample (Fig. 2(b)) confirmed the presence of thiol groups by observing the bands at 2550 cm^{-1} (S-H symmetric stretching vibration) (17). However, the peak for the S-H stretching vibration was too small to be specific to the thiol group. This is most probably due to the relatively low thiol concentration on the polymer beads together with the low

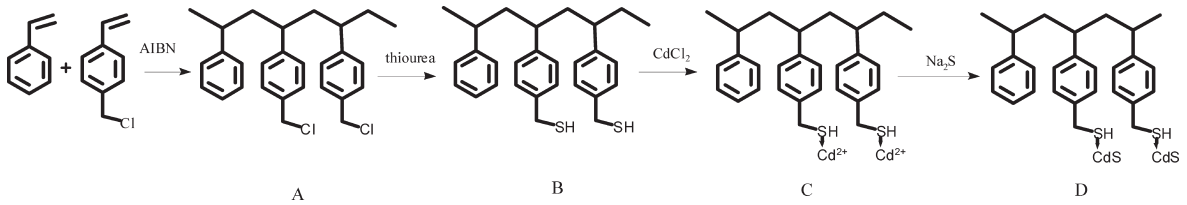

Fig. 1. Flow chart of synthesis of TPSC nanocomposites. (A: Polystyrene-co-polychloromethylstyrene; B: TPS; C: TPS-Cd^{2+}; D: TPSC).

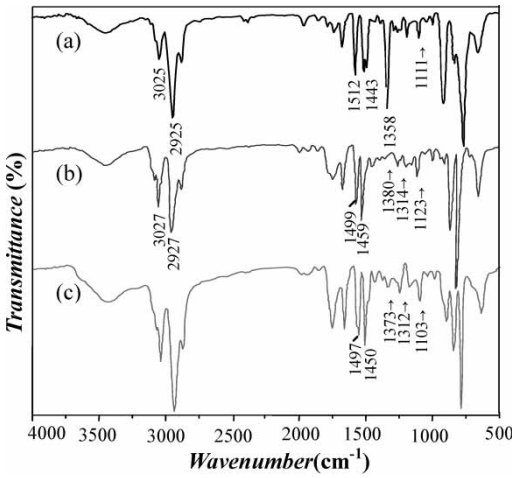

Fig. 2. FT-IR spectra of (a) polystyrene-*co*-polychloromethylstyrene; (b)TPS and (c) TPSC.

extinction coefficient of this vibration (18, 19). The absorption peak of 1459, 1499 cm^{-1} in spectrum (b) for TPS changed to 1450, 1497 cm^{-1} (TPSC). It is well known that 1450, 1497 cm^{-1} are the absorption peak of the phenyl group ($\delta_{C\text{-}H}$), indicating the S-Cd vibrations of SH → CdS groups (20).

3.3 Raman Spectra

Raman spectroscopy is more sensitive towards S–H vibration than FT-IR technique. TPS (Fig. 3(a)) and TPSC (Fig. 3(b)) exhibit the characteristic C-H binding at 2910–3049 cm^{-1} and S-H binding at 2563–2574 cm^{-1} (21). In addition, the Raman bands at 1234 assigned to CH_2-S were observed. The peak at 999–1031 cm^{-1} in TPS disappeared when TPS stabilizes CdS nanoparticles. The Raman results clearly show the existence of thiol groups and the thiols stabilize CdS nanoparticles via S-Cd bonding (22).

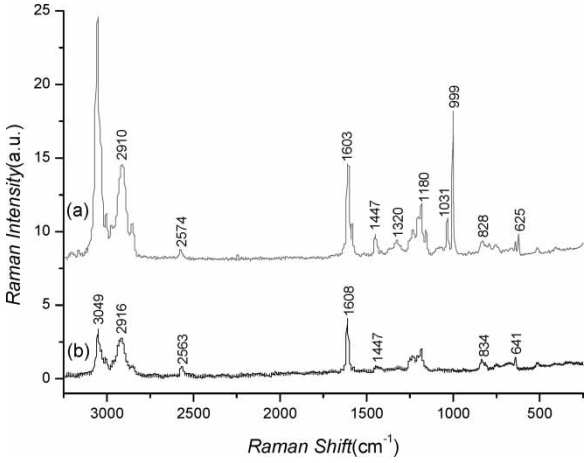

Fig. 3. FT-Raman spectra of (a) TPS and (b) TPSC.

3.4 ^{1}H-NMR Spectra

Figure 4 shows a ^{1}H-NMR spectrum of PSt-$(CH_2Cl)_x$, TPS and TPSC. The protons of -CH_2-Cl groups in PSt-$(CH_2Cl)_x$ (Fig. 4(a)) can be found at 4.51 ppm (23). In TPS and TPSC (Fig. 4(b) and (c)), the chemical shift at 2.96 ppm was assigned to the protons on the methylene carbons adjacent the sulfur atom (-CH_2-S-) (24), the production of the TPSC composite could be confirmed.

3.5 XPS, SEM and ICP Analysis

Conversion of the chlorine side-group into thiol in TPS and the formation of –SH → CdS complex were again confirmed by XPS spectroscopy (Fig. 5). The appearance of a characteristic Cd 3d5/2 peak at 404.5 eV, S 2p peak at 161.8 eV confirms the existence of cadmium and sulfur species in the TPSC. In addition, XPS data also allows the determination of atomic ratios between S and Cd from the particles (25). The S/Cd atom number ratio was 2.16:1 in the TPSC, which was consistent with the results of SEM (S/Cd = 2.12:1). The molecular weight of TPS was calculated by ICP-XPS and ^{1}H-NMR analysis:

$$M_n = (n_S/n_{Cd}) \times C_{Cd}[150 + 104(I_{6.852-7.348}/I_{6.556-6.750})] \quad (1)$$

Where n_S and n_{Cd} were of S/Cd atom number ratio (XPS); C_{Cd} was the content of Cd (mol/g, ICP); $I_{6.556-6.750}$ and $I_{6.852-7.348}$ were the integral value of $\delta = 6.556$–6.750 ppm and $\delta = 6.852$–7.348 ppm (^{1}H-NMR) respectively; the 104 and 150 were of the molecular weight (g/mol) of styrene and PSt-CH_2SH, respectively.

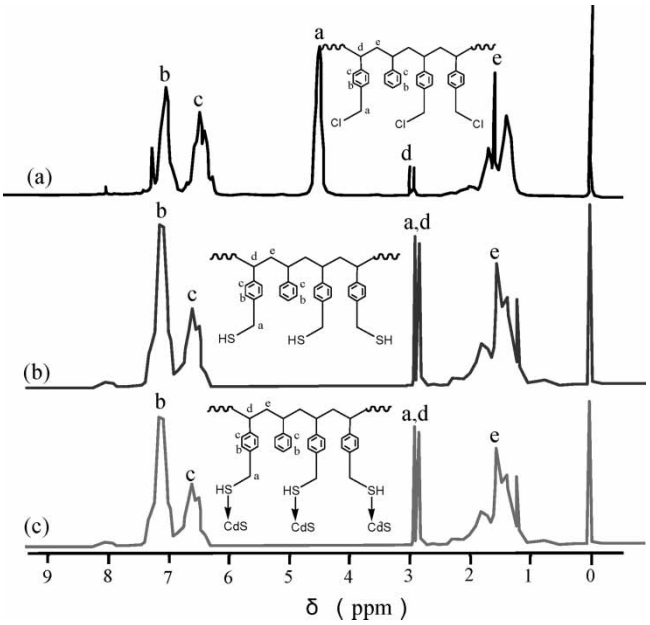

Fig. 4. ^{1}H-NMR spectra of (a) polystyrene-*co*-polychloromethylstyrene; (b) TPS and (c) TPSC.

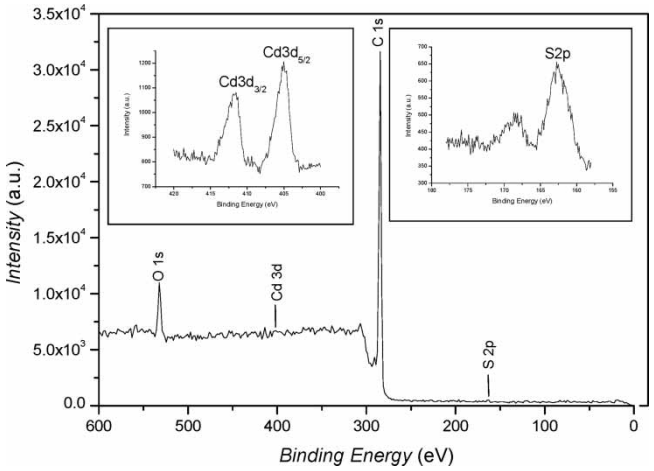

Fig. 5. XPS spectra of TPSC. The inset shows enlarged binding energy curves of S 2p, Cd $3d_{3/2}$ and Cd $3d_{5/2}$.

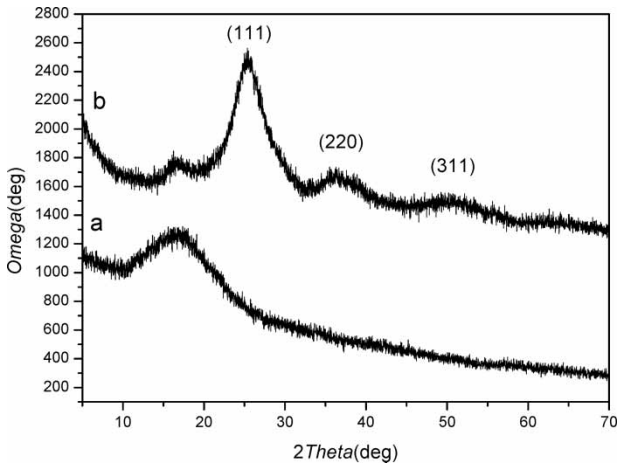

Fig. 7. XRD patterns of samples (a) TPS and (b) TPSC.

3.6 TGA/DSC Analysis

Thermal stability of samples were investigated by TGA/DSC (Fig. 6). The initial mass loss of 5%-to-decomposition endotherms of polystyrene-*co*-polychloromethylstyrene, TPS and TPSC are observed at 430.17, 422.49–442.13 and 418°C, respectively. The complete decomposition of samples (weight loss range from 94.97% to 84.20% at 600°C) occurs as depicted in Fig. 6. This indicates that the degradation of TPSC is a slow process. The presence of CdS in the polymer chain could be responsible for the enhanced decomposition of polymer-cluster nanocomposite (26). The nanocomposites TPSC contains 10.7% of CdS and 89.3% of organic component (27), which is consistent with XPS and SEM analysis.

3.7 XRD Patterns

XRD patterns of TPS and TPSC are shown in Fig. 7. The diffraction peak (Fig. 7(a)) at $2\theta = 19.06^\circ$ corresponds to amorphous TPS. The peaks at 2θ values of 26.48°, 43.68° and 51.4° (Fig. 7(b)) match the (111), (220) and (311) crystalline planes of cubic CdS. This microcrystal state showed not only the characteristic of the CdS crystal, but also the broad dispersion of diffraction peak. The average diameter of CdS particles was estimated to be about 2.2 nm according to the Debby–Scherer's equation (28):

$$L_{hkl} = k\lambda/B\cos\theta \qquad (2)$$

where k was taken as 1, $\lambda = 0.15418$ nm and B was half the width of the diffraction peak.

3.8 TEM Micrograph

TEM was employed to study the structures of nanocomposites. As evidenced from TEM images (Fig. 8(A)), TPSC composites are microsphere. Nano CdS is enwrapped by TPS. The inset of Fig. 8(A) shows a narrow dispersion of TPSC nanocomposites. The average size of the CdS nanocrystals are ranging from 2 to 3 nm (Fig. 8(B)). The polymer matrix plays an important role in controlling the morphology and distribution of nanoparticles.

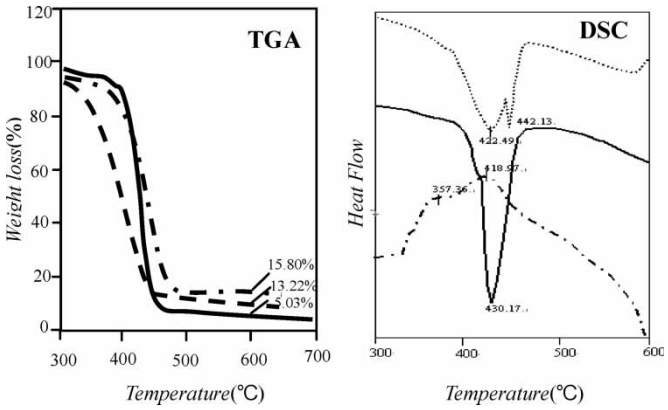

Fig. 6. TGA/DSC measurements of (···) polystyrene-*co*-polychloromethylstyrene; (_) TPS and (—·—) TPSC.

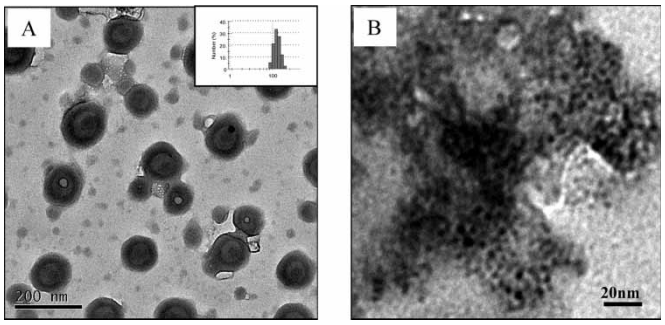

Fig. 8. TEM micrograph of (A) TPSC nanocomposites and (B) Enlarged image of TPSC nanocomposites.

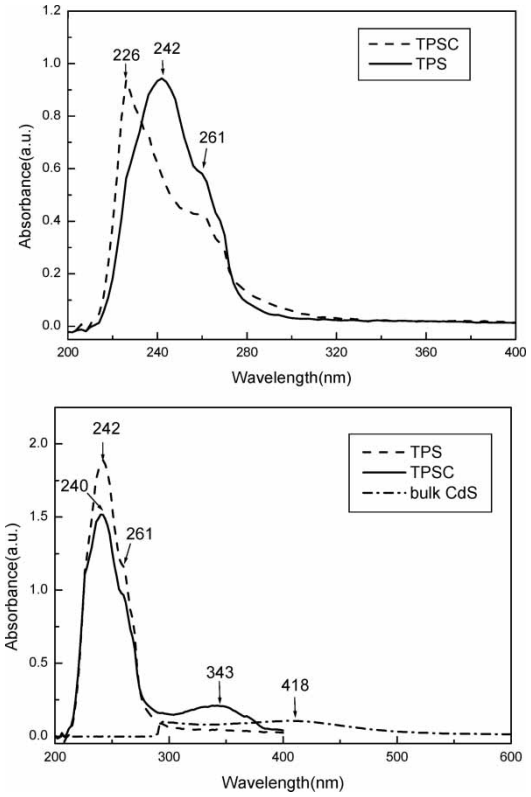

Fig. 9. UV-Vis spectra of bulk CdS, TPS, and TPSC with different CdS content in TPSC: 0.23×10^{-2} mol/g, up; 3.43×10^{-2} mol/g, down.

3.9 UV-Vis Absorbance Spectra

UV-Vis absorption of TPS and TPSC nanocomposites were recorded in Fig. 9. The maximum absorption peak at 226 and 242 nm (Fig. 9 (left)) are assigned to the optical transition of the first excitation state in TPS and TPSC, respectively. The obvious blue shift of the absorption peak of TPSC can be attributed to the quantum effect of CdS (29–31). In a

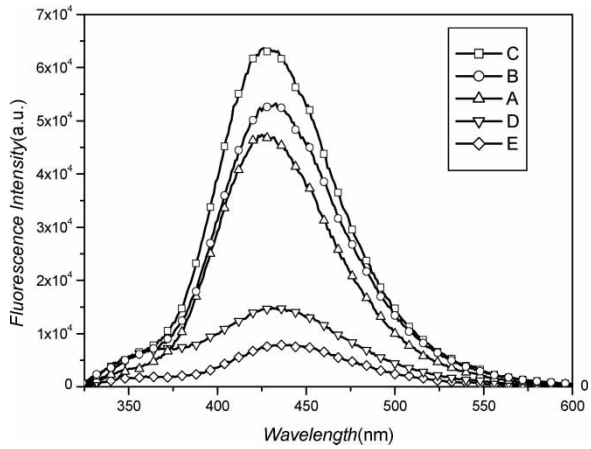

Fig. 11. The effect of CdS content on the fluorescence of TPSC: (A) 0.56; (B) 0.87; (C) 1.03; (D) 1.56 and (E) 2.31×10^{-2} mol/g.

absorption peak at 343 nm is assigned to nano CdS. In comparison, Fig. 9 (right, CdS/TPSC $= 3.43 \times 10^{-2}$ mol/g) with Fig. 9 (left, CdS/TPSC $= 0.23 \times 10^{-2}$ mol/g), we can see that the absorption of TPSC exhibits a red shift along with an increasing CdS content.

3.10 PL Properties

The ratio of band edge to deep trap emission, the spectral position, the absolute intensity, as well as the lifetimes, can be strongly influenced by particle size and surface characteristics (32). In this work, TPS and TPSC were dissolved in purified DMF and the PL spectra were obtained at room temperature. Meanwhile, the products films were prepared by a spin-coated method and the PL properties also were examined. Results show that PL intensity of TPSC is much stronger than that of TPS both in DMF solution (Fig. 10, left) and in film (Fig. 10, right). The marked peaks of TPSC blue-shifted from 443 nm (TPS) to 433 nm (Fig. 10, left). The nanocomposites showed significantly enhanced

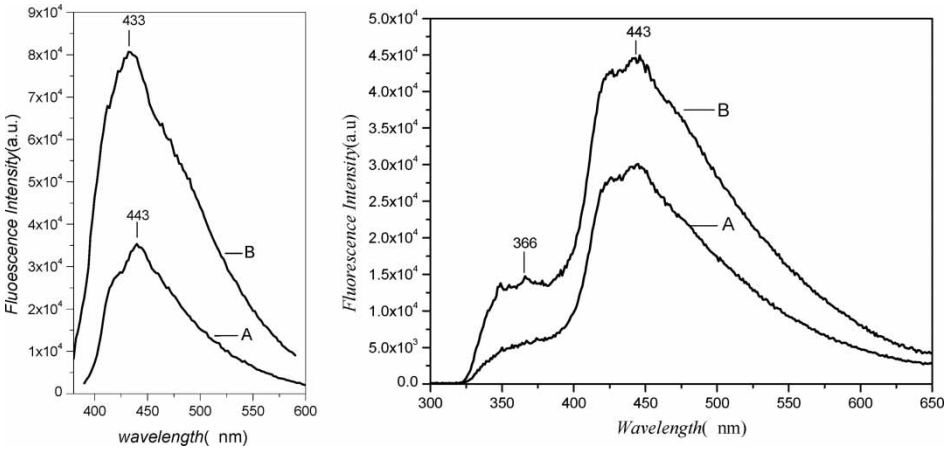

Fig. 10. Photoluminescence spectra of (A) TPS and (B) TPSC: left, DMF solutions, 10 mg/10 ml, $\lambda_{ex} = 373$ nm; right, films, $\lambda_{ex} = 322$ nm.

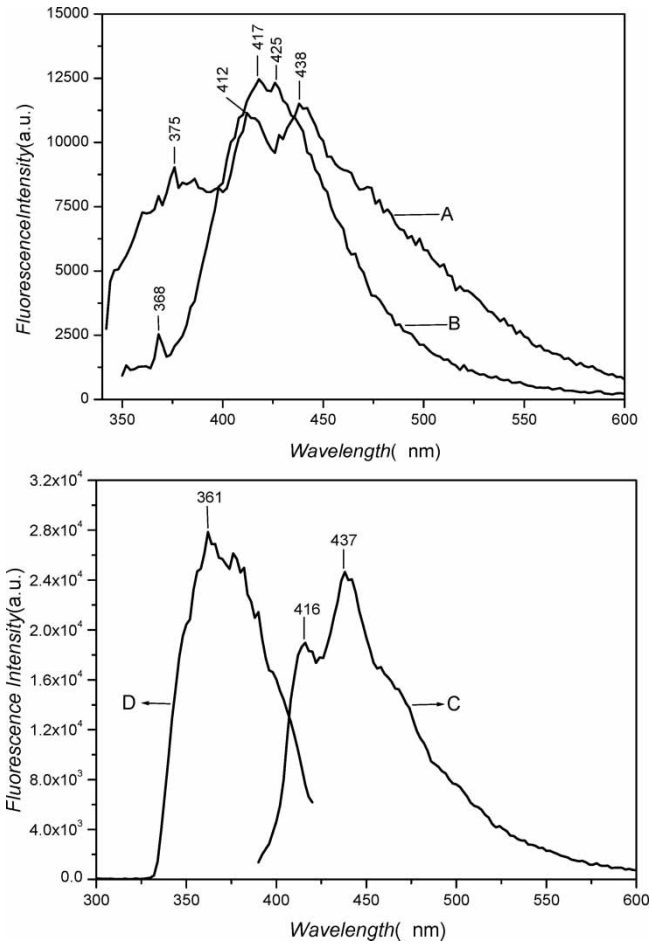

Fig. 12. The photoluminescence spectra: (A) CdS; (B) TPSC with excited wavelength of CdS ($\lambda_{ex} = 322$ nm); (C) TPSC and (D) CdS with excited wavelength of TPS ($\lambda_{ex} = 361$ nm).

luminescence property compared with that of the noncapped ones. We attributed this observation to the quantum effect of the CdS nanoparticles (33–36).

The effect of CdS content on fluorescence of TPSC was also investigated. CdS content was controlled by the amount of thiol which was confined by the copolymerization of styrene and chloromethylstyrene. Figure 11 shows that the PL intensity is enhanced by increasing the CdS content from 5.6 to 23.1 mmol/g TPSC. The red-shift PL peaks are observed with the increasing CdS content. This can be assigned to the formation of large particles or agglomerates (37).

The fluorescence efficiency (ϕ) obtained by the method is mentioned in the literature (38). The fluorescence efficiency ranked as TPSC (0.32), TPS-Cd^{2+}(0.30), TPS (0.18) due to the volume effect and surface effect of nano CdS.

The charge-transfer process between fluorophores and nano-CdS can be interpreted by the mechanism of metal-centered charge-transfer (MCCT), ligand-centered charge-transfer (LCCT), metal-to-ligand charge-transfer (MLCT) and ligand-to-metal charge-transfer (LMCT) (39). In our current work, the PL spectra of TPSC and CdS are obtained using an excitation wavelength of 322 nm (excitation wavelength of CdS) (Fig. 12, A, B) and 361 nm (excitation wavelength of TPS) (Fig. 12, C, D), respectively. There are two broad peaks at 438 and 412 nm for bulk CdS and two narrow peaks at 425 and 417 nm for TPSC. The blue shift from 438 to 417 indicates the quantum effect of the CdS nanoparticles incorporated with TPS (Fig. 12, left). With the excitation wavelength of 361 nm, PL spectrum of TPSC shows the strongest peak at 437 nm and a shoulder at 416 nm (CdS) relative to the emission of TPS (443 nm). Results indicate that changing the excitation wavelength affected the intensity ratio of the two peaks in the emission spectrum, but not their positions (40). Therefore, we can presume that the charge-transfer mechanism of TPSC should be a LMET model.

4 Conclusions

In this article, thiol-functional polystyrene-CdS nanocomposites have been successfully prepared via an *in-situ* method. The nanocomposites were characterized in detail. Results show that the content of CdS assume the effect on the PL performance. The amount of thiol can be controlled by the copolymerization of styrene and 4-chloromethylstyrene, so the CdS content in TPSC was confined by *in-situ* synthesis quantitatively. The study also indicates that the charge-transfer mechanism agrees with the ligand-to-metal charge-transfer model. These nanocomposites can be used as potential optical materials.

5 Acknowledgments

The authors appreciate the generous financial support of this work from the National Nature Science Foundation of China (20476066 and 20571054) the NSF of Jiangsu Province (BK2005031) and project of high technology of Jiangsu Province (BG2005021).

6 References

1. Bawendi, M.G., Steigerwald, M.L. and Brus, L.E. (1990) *Annu. Rev. Phys. Chem.*, **41**, 447.
2. Wang, Y. (1991) *J. Phys. Chem.*, **95**, 525.
3. Lianos, P. and Thomas, J.K. (1986) *Chem. Phys. Lett.*, **125**, 299.
4. Chen, W., Lin, Z., Wang, Z. and Lin, L. (1996) *Solid State Commun.*, **100**, 101.
5. Chang, L.T. and Yen, C.C. (1995) *J. Appl. Polym. Sci.*, **55**, 371.
6. Alivisatos, A.P. (1996) *Science*, **27**, 933.
7. Beecroft, L.L. and Ober, C.K. (1997) *Chem. Mater.*, **9**, 1302.
8. Antonietti, M. (1998) *Adv. Mater.*, **10**, 195.
9. Shiojiri, S., Irai, T. and Komasawa, I. (1998) *J. Chem. Soc., Chem. Commun.*, **21**, 439.
10. Murakoshi, K., Hosokawa, H., Saitoh, M., Wada, Y., Sakata, Mori, T.H., Satoh, M. and Yanagida, S. (1998) *J. Chem. Soc., Faraday Trans.*, **94**, 579.

11. Schmitt-Rink, S., Chemla, D.S. and Miller, D.A.B. (1989) *Adv. Phys.*, **38**, 89.
12. Khanna, P.K., Lonkar, S.P., Subbarao, V.V.V.S. and Jun, K.-W. (2004) *Mater. Chem. Phys.*, **87**, 49.
13. Faul, C.F.J., Antonietti, M., Hentze, H.P. and Smarsly, B. (2003) *Colloids Surf. A, Physicochem. Eng. Aspects*, **212**, 115.
14. Talapin, D.V., Poznyak, S.K., Gaponik, N.P., Rogach, A.L. and Eychmüller, A. (2002) *Physica E*, **14**, 237.
15. Hirai, T., Saito, T. and Komasawa, I. (2000) *J. Phys. Chem. B*, **104**, 11639.
16. Carrot, G., Scholz, S.M., Plummer, C.J.G. and Hilborn, J.G. (1999) *Chem. Mater.*, **11**, 3571.
17. Garamszegi, L., Donzel, C., Carrot, G., Nguyen, T.Q. and Hilborn, J.l. (2003) *React. Funct. Polym.*, **55**, 179.
18. Phan, K.X., Cho, M., Nam, J.-D. and Lee, Y. (2006) *Synth. Met.*, **156**, 872.
19. Zhang, L. and Chen, Y. (2006) *Polymer*, **47**, 5259.
20. Berkel, P.M., Driessen, W.L., Reedijk, J., Sherrington, D.C. and Zitsmanis, A. (1995) *React. Funct. Polym.*, **27**, 15.
21. Wang, C.C., Chen, A.L. and Chen, I.H. (2006) *J. Colloid. Interf. Sci.*, **293**, 421.
22. Yang, Q., Liu, J., Yang, J., Zhang, L., Feng, Z., Zhang, J. and Li, C. (2005) *Micropor. Mesopor. Mat.*, **77**, 257.
23. Zhang, L. and Chen, Y. (2006) *Polymer*, **47**, 5259.
24. Kim, J., Kim, S.S., Kim, K.H., Jin, Y.H., Hong, S.M., Hwang, S.S., Cho, B.-G., Shin, D.Y. and Im, S.S. (2004) *Polymer*, **45**, 3527.
25. Zhang, H., Zhou, Z. and Yang, B. (2003) *J. Phys. Chem. B*, **107**, 8.
26. Yan, B., Chen, D. and Jiao, X. (2004) *Mater. Res. Bull.*, **39**, 1655.
27. Sonar, P., Sreenivasan, K.P., Madddanimath, T. and Vijayamohanan, K. (2006) *Mater. Res. Bull.*, **41**, 198.
28. Pan, L.J., Chen, D.Z. and He, P.S. (2004) *Mater. Res. Bull. (USA)*, **39**, 243.
29. Chen, C., Zhu, C., Hao, L., Hu, Y. and Chen, Z. (2004) *Inorg. Chem. Commun.*, **7**, 322.
30. El-Tantawy, F., Abdel-Kader, K.M., Kaneko, F. and Sung, Y.K. (2004) *Euro. Polym. J.*, **40**, 415.
31. Hirai, T., Saito, T. and Komasawa, I. (2000) *J. Phys. Chem. B*, **104**, 11639.
32. Wu, F., Zhang, J.Z., Kho, R. and Mehr, R.K. (2000) *Chem. Phys. Lett.*, **330**, 237.
33. Liu, S.H., Qian, X.F., Yin, J., Ma, X.D., Yuan, J.Y. and Zhang, Z.K. (2003) *J. Phys.Chem. Soli.*, **64**, 455.
34. Sakai, H., Itaya, A. and Masuhara, H. (1996) *Polymer*, **37**, 31.
35. Kim, S. and Inglett, G.E. (2006) *J. Food Compos. Analy.*, **19**, 466.
36. Lu, L., Helgeson, R. and Jones, R.M. (2002) *J. Am. Chem. Soc.*, **124**, 483.
37. Carrot, G., Scholz, S.M., Plummer, C.J.G. and Hilborn, J.G. (1999) *Chem. Mater.*, **11**, 3571.
38. Nair, P.S., Radhakrishnan, T.N., Revaprasadu, N., Kolawole, G.A. and Brien, P.O. (2002) *Chem. Commun.*, **10**, 564.
39. Jiang, Y.S. and Yang, W.S. *Electronic Process in Chemistry*; Science Press: Beijing, China, 209, 2004.
40. Carrot, G.S., Scholz, M., Plummer, C.J.G. and Hilborn, J.G. (1999) *Chem. Mater.*, **11**, 3571.